

Crystalline Isotactic *trans*-1,4-Poly(penta-1,3-diene). A New Approach to Conformational and Packing Energy Evaluation

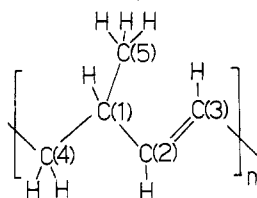
D. R. Ferro[†] and S. Brückner^{*‡}

Istituto di Chimica delle Macromolecole del CNR, Via E. Bassini, 15, 20133 Milano, Italia, and Dipartimento di Chimica del Politecnico di Milano, Piazza Leonardo da Vinci, 32, 20133 Milano, Italia. Received April 25, 1988; Revised Manuscript Received October 25, 1988

ABSTRACT: Conformational and packing energy of crystalline isotactic *trans*-1,4-poly(1,3-pentadiene) has been analyzed with a computational procedure where both intra- and intermolecular interactions are simultaneously taken into account within each minimization cycle. This methodological improvement affords results in substantial agreement with the model directly refined on the powder X-ray diffraction profile. The discriminating power of the observed profile toward different theoretical models of the polymer crystal structure is also investigated.

Introduction

The crystal structure of isotactic *trans*-1,4-poly(1,3-pentadiene) (ITPP) has been widely studied by a number



ITPP

of researchers, both by experimental X-ray diffraction^{1,2} and vibrational analysis³ and by molecular modeling based on conformational and packing energy minimizations.^{4,5} The reason for this interest is probably due to the fact that the two distinct conformations available to the polymer chain find experimental evidences supporting their presence in the crystalline state. The two conformations are not isoenergetic for an isolated chain; the most stable one locates the side methyl group in a skew orientation relative to the nearest double bond (skew conformation) while a higher conformational energy is required to locate the methyl group in the plane defined by the nearest double bond and the tertiary carbon atom (cis conformation).⁴

X-ray diffraction and vibrational analysis data, both collected on crystalline unstretched samples, agree in assigning the skew conformation to the polymer chain.^{2,3} An X-ray diffraction study carried out on data collected from oriented fibers shows a better semiquantitative agreement when the cis conformation is adopted.¹ It is worthwhile mentioning also that the cis conformation has been observed in low molecular weight model compounds.⁶

In the most recent experimental study the authors reported strong evidence indicating that the two sets of diffraction data, the one obtained from the oriented fiber and the one obtained from the unstretched polymer are *mutually incompatible*.² As a consequence it is necessary to postulate the existence of a conformational change partially or completely induced by stretching the polymer at a temperature close to the melting point (ca. 100 °C).

In a subsequent paper by Napolitano⁵ the problem was tackled from the point of view of conformational and packing energy minimization. The procedure adopted is substantially that of optimizing the conformation of an isolated chain (obeying a given periodicity along the chain axis) and performing, in a successive step, a rigid-body adjustment within the unit cell to find the most efficient

packing of a number of chains subjected to a given space symmetry. An absolute minimum was found that indeed corresponds to the skew conformation but has the chain axis significantly displaced from the position refined on powder X-ray diffraction data and quite close to the position refined, for the cis conformation, on oriented fiber X-ray diffraction data. Such a result might induce one to consider this model as a possible compromise satisfying both sets of experimental data, discarding the hypothesis of a stretching-induced transition to the cis conformation.

The idea of comparing a structural model refined on experimental data with models refined on the basis of a theoretical force field can be fruitful particularly when, as in this case, experimental data are of modest quality and leave margins of uncertainty about details of the refined geometry. High accuracy and general validity of results may however be obtained, in our opinion, only if the computational procedure is planned to keep at minimum arbitrary assumptions (e.g., the spherical symmetry of methyl groups) while improving the realistic aspects of the model to the best level compatible with the computer at hand. The force field adopted should be self-consistent without any ad hoc parameter adjustment; both intra- and intermolecular interactions are to be taken into account within the same optimization cycle, and all atoms involved (hydrogens included) should contribute explicitly to the total energy. Along this line we decided to reconsider the problem of conformation and crystal packing of ITPP by utilizing the program REFIN⁷ for energy minimization of macromolecular systems. One feature of this program allows one to carry the minimization procedure by adjusting all or part of the atomic Cartesian coordinates of a microcrystal, whose size can be arbitrarily fixed, taking into account *simultaneously* both intra- and intermolecular interactions of a given asymmetric unit with the surrounding symmetric ones.

For the present work Allinger's MM2 force field⁸ was adopted, with the minor difference that the torsional energy is computed, at each bond, by means of a single-term function, best-fitted to Allinger's combination of several terms. A cutoff limit of 6 Å was chosen, meaning that all atoms of one unit interact with all atoms of another unit if at least one pair of atoms are within the limit. This means that, in practice, many interactions beyond the cutoff limit are taken into account as well. No geometrical constraints were imposed on the atomic coordinates, except for keeping the unit cell dimensions equal to the observed values. For practical reasons the same nonbonded parameters were utilized for both intra- and interchain interactions, although according to our experience two distinct potential sets would be required for a proper simulation of thermal expansion. We feel that, while the use

[†] Istituto di Chimica delle Macromolecole del CNR.

[‡] Dipartimento di Chimica del Politecnico di Milano.

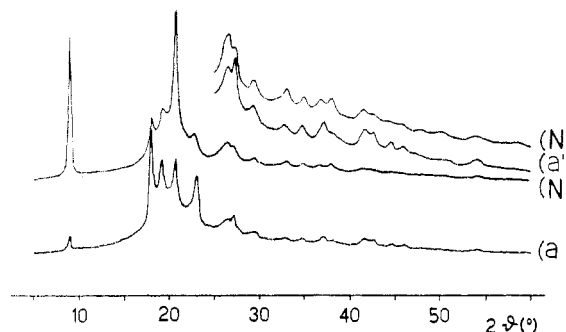


Figure 1. Comparison of the observed profile of ITPP (curve a) and the profile calculated with model N (see text) labeled with the same letter. Curves a' and N' are the same as a and N on an enhanced scale.

of more appropriate intermolecular nonbonded potentials (see, for example, the recent OPLS parameters by Jorgensen⁹) is necessary when energy is minimized *also with respect to the unit cell dimensions*, the effects of our choice are much less relevant in the present study. The procedure adopted here¹⁰ represents, in our opinion, a methodological improvement relative to the previous study of Napolitano, and the results obtained are worthwhile for a discussion focused both on the discriminating power of the observed powder profile with regard to the location of the chain axis within the unit cell and on the consequences of the improvements adopted in the determination of the absolute minimum of the crystal structure. Since the minimum we find is quite close to the model that best fits the powder diffraction data and, as already stated, the quality of the observed profile is modest, the final discussion will also deal with the possibility of merging some relevant aspects of the theoretical geometry into the crystallographic structure without losing too much in the goodness of fit computed on the observed data.

Results

Our first intention was to enquire on the ability of the model proposed by Napolitano (model N) to reproduce the shape of the observed powder profile. This model was obtained in a unit cell having dimensions equal to those measured at room temperature while the most detailed profile was recorded at -120°C , a temperature that determines a small contraction along a and b .² However the differences involved consist only in small deviations of the peak positioning on the 2θ scale; hence the profile calculated with model N and cell dimensions detected at room temperature can be compared with the profile recorded at -120°C . The discrepancies induced by differences in the cell dimensions are actually of little importance when compared with the much stronger effects exerted on the calculated intensities by the proposed positioning of atoms in the unit cell. Figure 1 shows these effects and also indicates that the most striking discrepancies are detected in the middle to low 2θ range ($2\theta < 25^{\circ}$), particularly sensitive to the location of the overall electronic density within the cell. For example, we recall that an outstandingly strong peak (210 ; $2\theta = 20.8^{\circ}$) was also present in the profile calculated with the model proposed by Bassi et al.¹ and approximately located in the same position of model N.² It is just this location of the chain axis, substantially irrespective of a cis or a skew conformation of the polymer chain, that determines the intensity of the (210) reflection, and therefore it cannot be accepted as a possible solution of the crystallographic problem represented by the unstretched polymer.

A second task was that of investigating the packing forces present in the crystal and their effects in the de-

Table I
Optimized Geometries and Energy Data of ITPP Isolated Chains in Skew and Cis Conformations

	skew ^a	skew	cis ^a	cis
Bond Angles, deg				
C(1)–C(2)–C(3)	124.1	124.0	125.9	124.6
C(2)–C(1)–C(4)	110.3	110.1	111.5	109.9
C(2)–C(3)–C(4)	123.7	123.5	124.6	123.4
C(1)–C(4)–C(3)	112.0	111.8	113.5	111.7
C(4)–C(1)–C(5)	111.8	111.8	112.8	113.1
C(2)–C(1)–C(5)	109.1	109.3	113.6	113.7
Torsion Angles, deg				
C(4)–C(1)–C(2)–C(3)	–119.2	–117.7	107.8	96.9
C(1)–C(2)–C(3)–C(4)	–177.4	–177.4	176.9	177.6
C(2)–C(3)–C(4)–C(1)	118.3	116.8	–106.8	–96.1
C(3)–C(4)–C(1)–C(2)	178.6	178.5	–177.8	–178.5
axial repeat, Å	4.85	4.83	4.85	4.72
energy, kcal/mol	2.45	2.43	3.77	3.41

^a These conformers have been obtained under the constraint of a given (4.85 Å) repeat period along the chain axis.

termination of the model of minimum energy. To check the compatibility of Allinger's force field with force fields already adopted in previous studies on polypentadiene,^{4,5} we minimized the conformational energy of the isolated chain in skew and cis conformations both with and without the action of a constraint on the elongation of the monomer to match the crystalline c axis (4.85 Å). Results are given in Table I, and it is worthwhile mentioning that the stabilization by 1.3 kcal/mol of the skew conformation relative to the cis one seems to be more realistic than the 2.8 kcal/mol calculated by Napolitano and the 2.3 kcal/mol calculated by one of the authors.⁴ In fact we recall that a cis conformation has indeed been found in single-crystal X-ray diffraction analyses of low molecular weight model compounds,⁶ and therefore the energy involved in this arrangement cannot be much higher than that pertaining to the skew conformation. Independent minimizations were performed on the chain surrounded by symmetry-related neighbors. Cell dimensions corresponding to $T = -120^{\circ}\text{C}$ ($a = 19.59$, $b = 4.75$, $c = 4.86$ Å) were assumed in order to allow for an immediate comparison with the observed profile, but the same calculations were afterward repeated in the cell measured at room temperature ($a = 19.80$, $b = 4.80$, $c = 4.85$ Å) to allow for a direct comparison with results obtained by Napolitano. We can anticipate however that no significant change was observed by varying the cell dimensions except for an almost uniform shift of the total energy (ca. 0.15 kcal/mol) to slightly lower values in the smaller cell.

We label the model that best fits the powder profile with A and summarize some features of this structure in Table II, while more details are available in ref 2. Model A was taken as the starting point for two independent minimization processes designed to establish the role played by hydrogens. In one calculation hydrogen atoms were adjusted first and then both carbons and hydrogens were refined together to the final geometry; in a subsequent calculation all atom positions were refined in a single-step procedure. This was an attempt to avoid possible trapping within secondary minima, a rather common event when the function to be minimized depends on a large number of variables. The way out usually adopted is that of doing a number of runs changing the starting point or the minimization path. This leads usually to final geometries characterized by small differences in the coordinates, a drawback that does not call in question the uniqueness of the minimum and is anyhow largely compensated for by the advantage of keeping at minimum arbitrary assump-

Table II
Summary of the Relevant Features of Structure A^a
Fractional Coordinates of Carbon Atoms

	<i>x</i>	<i>y</i>	<i>z</i>
C(1)	0.1143	0.1842	-0.1907
C(2)	0.1104	0.0198	0.0718
C(3)	0.0881	0.1507	0.2994
C(4)	0.0875	-0.0028	-0.4268
C(5)	0.1893	0.2661	-0.2416

Bond Angles, deg			
C(1)-C(2)-C(3)	118.6	C(1)-C(4)-C(3)	112.0
C(2)-C(1)-C(4)	108.6	C(4)-C(1)-C(5)	110.5
C(2)-C(3)-C(4)	120.3	C(2)-C(1)-C(5)	108.6

Torsion Angles, deg			
C(4)-C(1)-C(2)-C(3)	-138	C(2)-C(3)-C(4)-C(1)	136
C(1)-C(2)-C(3)-C(4)	-176	C(3)-C(4)-C(1)-C(2)	178

^a See ref 2 for more details.

Table III
Some Relevant Features of Structure B
Fraction Coordinates of Carbon Atoms

	<i>x</i>	<i>y</i>	<i>z</i>
C(1)	0.1174	0.1284	-0.1872
C(2)	0.1154	-0.0189	0.0885
C(3)	0.0842	0.0842	0.3126
C(4)	0.0858	-0.0589	-0.4095
C(5)	0.1919	0.2042	-0.2551

Bond Angles, deg			
C(1)-C(2)-C(3)	124.1	C(1)-C(4)-C(3)	112.4
C(2)-C(1)-C(4)	110.4	C(4)-C(1)-C(5)	111.8
C(2)-C(3)-C(4)	123.3	C(2)-C(1)-C(5)	109.1

Torsion Angles, deg			
C(4)-C(1)-C(2)-C(3)	-121.2	C(2)-C(3)-C(4)-C(1)	120.2
C(1)-C(2)-C(3)-C(4)	-176.7	C(3)-C(4)-C(1)-C(2)	177.7

Chain Axis Position (Fractional Coordinates) and Displacement Relative to Structure A

<i>x</i> = 0.1007	Δx = 0.0006
<i>y</i> = 0.0337	Δy = -0.0543

Energy, kcal/mol

total energy = -5.576 (bonded 0.777, nonbonded -6.353)

tions about the geometry of the model.

In this case the two final structures are almost indistinguishable and quite close to the starting crystallographic model; we label this refined model with B and report in Table III some relevant features of this structure. A second attempt of checking for the uniqueness of minimum B was performed by rotating the chain by $\pm 10^\circ$ around an axis parallel to the chain direction and passing through the methyl group and then again minimizing the energy. The substantial result of these exploring calculations was that of revealing the presence of a shallow minimum around B; all deviations from the starting geometry in fact involved small energy differences while the recovery process led to minima that, on a very detailed scale, were slightly biased by the original deviation. As average uncertainties in the atomic positions were of the order of 0.05 Å, no doubt exists about uniqueness of minimum B. In Figure 2 we show a comparison of the observed profile (curve a) with the profile calculated with model B (curves B and B'). The agreement is, of course, worse than that calculated with structure A but good enough to reproduce the fundamental features of the profile in the whole 2θ range. In other words, from an opposite point of view, structure B could be a very convenient starting point, obtained with a mere computational procedure, without any ad hoc adjustment, for a crystallographic refinement.

The model refined by Napolitano was assumed then as the starting point in another group of minimization runs.

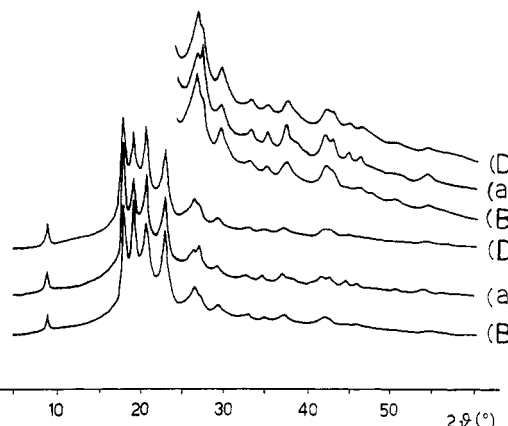


Figure 2. Comparison of the observed profile of ITPP (curve a) and the profiles calculated with model B and D (see text) labeled with the same letters. Curves a', B', and D' are the same as a, B, and D on an enhanced scale.

Table IV
Some Relevant Features of Structure C
Fractional Coordinates of Carbon Atoms

	<i>x</i>	<i>y</i>	<i>z</i>
C(1)	0.1154	0.2484	-0.2140
C(2)	0.1021	0.1179	0.0638
C(3)	0.0781	0.2568	0.2860
C(4)	0.0679	0.1242	-0.4362
C(5)	0.1909	0.2042	-0.2881

Bond Angles, deg			
C(1)-C(2)-C(3)	124.8	C(1)-C(4)-C(3)	112.9
C(2)-C(1)-C(4)	111.1	C(4)-C(1)-C(5)	111.3
C(2)-C(3)-C(4)	124.1	C(2)-C(1)-C(5)	108.9

Torsion Angles, deg			
C(4)-C(1)-C(2)-C(3)	-115.7	C(2)-C(3)-C(4)-C(1)	114.8
C(1)-C(2)-C(3)-C(4)	-177.2	C(3)-C(4)-C(1)-C(2)	178.3

Chain Axis Position (Fractional Coordinates) and Displacement Relative to Structure A

<i>x</i> = 0.0909	Δx = -0.0090
<i>y</i> = 0.1871	Δy = 0.1000

Energy, kcal/mol

total energy = -5.213 (bonded 1.066, nonbonded -6.279)

The minimum reached, labeled C, is rather close to the starting model and therefore quite distinct from model B; it is ca. 0.36 kcal/mol higher than B. The conformation in model C is, of course, skew, but a more detailed analysis revealed that in this case torsion angles deviate significantly from the theoretical values of $\pm 120^\circ$ obtained in the isolated chain and very closely reproduced in model B. In the case of model C, unlike model B, we are therefore in the presence of a rather important effect of packing on the conformation of the chain. In Table IV we report some features of model C.

A comparison of models B and C shows that they are shifted by about 0.15 Å along the chain axis while in the *a,b* plane the side methyl groups are almost coincident and the chain axes are displaced by 0.75 Å, nearly totally ascribed to the projection along *b*. Further investigation was devoted to analyze possible paths leading from one minimum to the other to get a better description of the characteristics of the energy hypersurface in the region. A transition from C to B was induced by a five-step procedure where the *x* and *y* coordinates of C(4) (see the structure of ITPP for the numbering scheme) were fixed at intermediate values and, at each step, a complete energy minimization was allowed. No significant barrier was detected along this path, but nevertheless we believe that the separation between C and B is not solely due to the

Table V
Some Relevant Features of Structure D
Fractional Coordinates of Carbon Atoms

	x	y	z
C(1)	0.1159	0.1747	-0.1934
C(2)	0.1128	0.0253	0.0802
C(3)	0.0837	0.1368	0.3045
C(4)	0.0837	-0.0042	-0.4198
C(5)	0.1909	0.2484	-0.2572

Bond Angles, deg

C(1)-C(2)-C(3)	123.6	C(1)-C(4)-C(3)	112.1
C(2)-C(1)-C(4)	110.2	C(4)-C(1)-C(5)	111.9
C(2)-C(3)-C(4)	123.0	C(2)-C(1)-C(5)	108.9

Torsion Angles, deg

C(4)-C(1)-C(2)-C(3)	-124.4	C(2)-C(3)-C(4)-C(1)	123.4
C(1)-C(2)-C(3)-C(4)	-176.7	C(3)-C(4)-C(1)-C(2)	177.8

Chain Axis Position (Fractional Coordinates) and Displacement Relative to Structure A

x = 0.0990	$\Delta x = -0.0011$
y = 0.0832	$\Delta y = -0.0047$

Energy, kcal/mol

total energy = -5.324 (bonded 0.628, nonbonded -5.951)

shallowness of the minimum and to the faint computational effects that this may involve. The physical meaning of the separation, which might require a very small and localized barrier, is testified to by the deviations from perfect skew torsions on the polymer chain in C (see Table III). Packing effects are to be invoked for this, and they must be removed to convert C into B where these deviations are absent, as indeed resulted in an appropriate minimization run.

The shallowness of the minimum, particularly with respect to changes in y and z , was already evident from data published by Napolitano⁵ and postulated by one of us in a paper concerning a possible explanation for the stretch-induced conformational transition,⁴ where the fundamental role played by side methyl groups in governing the packing features of the structure was pointed out together with the much weaker influences experienced by main-chain atoms. All proposed models in fact locate side methyl groups within a very narrow region in the unit cell and differ mainly in the position of the chain axis. Next we wanted to investigate on the relation of structure B with structure A, which corresponds to the crystallographic best fit with powder data. We did this by linking carbon atoms of structure A with their starting positions through an elastic potential where the force constant can be fixed at will and then performing minimization runs under the action of these artificial constraints. By a progressive weakening of the force constant it is thus possible to graduate the transition from A to B. This change occurs basically in two steps, roughly distinguished by the different energy changes involved. The first one is characterized by a conformational adjustment where the skew torsions are restored to nearly standard values; it accounts for ca. 70% of the total lowering in energy while atoms are displaced from their original positions by only 30% of the final average shift; we label this structure D. The second one determines an overall displacement of the main chain of about -0.18 Å, mainly projected along b , leading to structure B, the absolute minimum.

Structure D, for which we report some geometrical features in Table V, is interesting because it achieves a geometry close to standard values without losing too much in the crystallographic goodness of fit. On the other hand our packing analysis has not revealed any particular effect on the chain backbone that might justify the deviation from theoretical skew torsions present in structure A

Table VI
Crystallographic Goodness of Fit of the Structural Models Analyzed^a

model	R	R_L	R_H
A	0.116	0.109	0.129
B	0.177	0.172	0.187
D	0.120	0.102	0.156

^a The disagreement factor R is in the form $R = \sum |I_o| - |I_c| / \sum I_{net}$, where $I_{net} = I_o - I_{backgr}$, and in addition to its overall value we report also the two contributions R_L ($2\theta < 25^\circ$) and R_H ($2\theta \geq 25^\circ$).

($\pm 137^\circ$ instead of $\pm 120^\circ$). These considerations, together with the modest quality of the observed profile particularly at high 2θ values, suggest that structures A and D may be considered two estimates of the *real* structure of substantially comparable reliability; the differences in their geometries thus define the effective uncertainty affecting the structural determination based on X-ray diffraction data in this case, characterized by an observed profile with few details at high 2θ values.

In Figure 2 we also report the profile calculated with model D (curves D and D'), and it may be noted that the worsening of the agreement relative to model A (see Figure 2 of ref 2) is almost indistinguishable at first sight and is clearly revealed only through the computational comparison.

In Table VI we report a summary of the disagreement factors R , in the form of $R = \sum |I_o - I_c| / \sum I_{net}$, where $I_{net} = I_o - I_{backgr}$, for structures A, B, and D. Together with the overall R factors we also report the contribution from middle to low 2θ range ($2\theta < 25^\circ$), labeled R_L , and from higher 2θ range, labeled R_H . This may be helpful for a rough separation of the contributions to R into a part mainly due to wrong positioning in the cell (R_L) and a part sensitive to more local details of the structure (R_H).

Finally we checked the stability of the *cis* model in the crystalline state by minimizing the total energy of the model refined by Bassi et al. on oriented fiber X-ray diffraction data. The final structure was reached after few cycles and its energy is 1.7 kcal/mol higher than that of model B (skew model) with a further increment of ca. 0.4 kcal/mol relative to the difference between the energies of the isolated chains. This result is in qualitative agreement with that of Napolitano, who also found that packing effects enhance the energy difference between the two conformers.

Conclusions

The combined action of crystallographic refinement and of energy minimization with simultaneous variation of packing parameters and of chain conformation provides an accurate solution to the problem of the crystal structure of unstretched ITPP. Structure D in fact represents a very reasonable compromise between crystallographic best fit and minimum-energy requirements, while structures A and B, the two extremes representing respectively the best agreement with diffraction data and the minimum-energy situation, are close enough to each other to leave a narrow margin of variation of the structural parameters. The discriminating power of powder X-ray diffraction data among different theoretical models of crystalline ITPP is more accurately investigated. The middle to low 2θ region is highly sensitive to changes in the position of the chain axis; any proposal of a possible model is thus bound to locate the polymer chain very close to the position of model A. On the other hand, the higher 2θ region is of modest quality, with few and broad peaks, so that, only on this basis, details of the polymer structure are affected by significant uncertainties and additional information from

proper energy calculations is required.

The differences between geometries of the isolated chain and of the crystal model are small, as may be observed by comparing data reported in Table II with data reported in Table I (skew* model), but this does not reduce, in our opinion, the importance of taking into account simultaneously both intra- and intermolecular interactions in the packing refinement process applied to a flexible model. First of all the energy difference between model B and C is small enough (0.3 kcal/mol) to be easily influenced even by small changes in the model adopted. Second, we think the flexibility of the model to be very important in determining the path of the minimization process, since it allows for smoothing asperities on the energy hypersurface.

A number of calculations, performed in the region of the absolute minimum, ensures its uniqueness and confirms the preminent role played by side methyl groups in determining the packing features of the polymer crystal; main-chain atoms undergo less critical interactions and are particularly insensitive to displacements along the *b* direction.

Acknowledgment. This research has been partly supported by CNR Italy (progetto strategico "Metodologie cristallografiche avanzate").

Registry No. ITPP, 29191-23-9.

References and Notes

- (1) Bassi, I. W.; Allegra, G.; Scordamaglia, R. *Macromolecules* 1971, 4, 575.
- (2) Brückner, S.; Di Silvestro, G.; Porzio, W. *Macromolecules* 1986, 19, 235.
- (3) Neto, N.; Muniz-Miranda, M.; Benedetti, E. *Macromolecules* 1980, 13, 1302.
- (4) Brückner, S.; Luzzati, S. *Eur. Polym. J.* 1987, 23, 217.
- (5) Napolitano, R. *Macromolecules* 1988, 21, 622.
- (6) Corradini, P.; Frasci, A.; Martuscelli, E. *J. Chem. Soc. D* 1969, 778.
- (7) The original program REFINE was developed by J. Hermans and co-workers at the University of North Carolina. M. Ragazzi and D. R. Ferro at ICM derived a version REFINE/U for UNIVAC computers and a version REFINE/HP for HP/9000 computers, which was used for the present calculations.
- (8) Allinger, N. L.; Yuh, Y. H. *QCPE* 1980, 12, 395.
- (9) Jorgensen, W. L.; Tirado-Rives, J. *J. Am. Chem. Soc.* 1988, 110, 1657.
- (10) This work had just been completed when we became aware of a very recent article by R. A. Sorensen, W. B. Lian, and R. H. Boyd (*Macromolecules* 1988, 21, 194) who propose a method for predicting polymer crystal structures accounting for both *intra-* and *intermolecular* energy. Although differing in the choice of the independent variables, their method shares with ours the use of *simultaneous* minimization of all energy contributions without arbitrary geometrical assumptions.

Chelating Ability of Poly(vinylamine): Effects of Polyamine Structure on Chelation

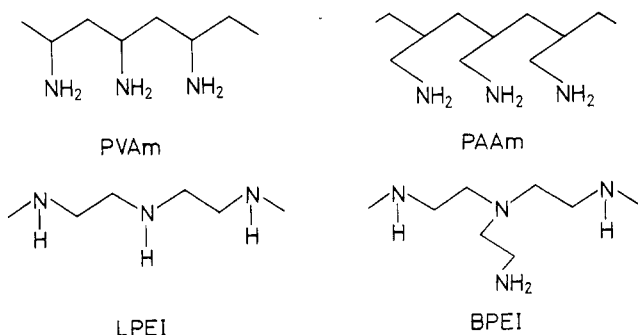
Shiro Kobayashi,* Kyung-Do Suh, and Yukio Shirokura

Department of Molecular Chemistry and Engineering, Faculty of Engineering, Tohoku University, Aoba, Sendai 980, Japan. Received August 1, 1988;
Revised Manuscript Received October 19, 1988

ABSTRACT: Chelating properties of poly(vinylamine) (PVAm) possessing the amino group linked directly to the main chain have been examined quantitatively for various heavy metal ions such as Co^{2+} , Ni^{2+} , Cu^{2+} , Zn^{2+} , and Cd^{2+} . Potentiometric titrations were performed and analyzed according to the modified Bjerrum method to give successive and overall stability constants, k_n and K_n , respectively. Two PVAm samples of different molecular weight were used for the chelate formation. The chelating ability of PVAm was compared with that of a polyamine, poly(allylamine) (PAAm), having one methylene group between the amino group and the main chain. The structural difference of PVAm and PAAm was shown from the dependency of the reduced viscosity on the pH value in the range of ionic strength $\mu < 1.0$. The difference in molecular weight of PVAm does not effect the chelate formation with heavy metal ions. From the K_n values, the chelating ability of PVAm was approximately 10–50 times less than that of PAAm for metal ions examined. Continuous variation analysis of the PVAm– Cu^{2+} complex examined by spectrophotometry revealed that the most stable complex is formed at $[\text{PVAm}]/[\text{Cu}^{2+}] = 4.0$.

Introduction

Polyamines form chelating complexes with various heavy metal ions. Recently, we have reported quantitative investigations on the chelating abilities of polyamines, linear and branched poly(ethylenimines) (LPEI and BPEI, respectively),¹ and poly(allylamine) (PAAm).² These three



polymeric amines provide very good polymer ligands

having different structures; i.e., LPEI has chelating sites only in the main chain,³ BPEI in both the main and side chains,^{4,5} and PAAm only in the side chain.⁶ On the other hand, poly(vinylamine) (PVAm) has only primary amino groups linked directly to the main chain. These four polyamines constitute a full set of polymer samples having different chelating sites due to the different microstructures. In a previous paper,¹ chelating properties of LPEI and BPEI have been studied to examine the influence of the microstructural difference of PEI (i.e., linear and branched structure) on the chelate formation. In this paper, the chelating ability of PVAm with various metal ions has been evaluated quantitatively by the determination of successive and overall stability constants with a potentiometric titration method and compared with that of PAAm. It is very significant that the chelating ability of four polyamines having different microstructures is evaluated on the basis of stability constants obtained by the same procedure in similar measurement conditions.^{1,2} Relevant to the present study, chelation between PVAm